REMARKS

In reply to the Office Action dated September 29, 2003, Applicants have amended the application as set forth above. Specifically, Claim 11 has been canceled without prejudice solely to advance the prosecution of the instant application. Claims 1, 3, 21, 25 and 26 have been amended. New Claims 28 and 29 have been added. Upon the entry of the amendments, Claims 1-10 and 12-29 are pending in this application. No new matter is added by the amendments as discussed below. Applicants respectfully request the entry of the amendments and reconsideration of the application in view of the amendments and the remarks set forth below.

Discussion of Amendments

Claim 1 has been amended to incorporate the limitations of Claim 11 and to further define the structure of the carbon molecular sieve. The amendments to Claim 1 are supported by, for example, the specification at page 3, lines 10-11 and 28-30, and page 4, lines 1-2. Claim 3 has been amended to correct a grammatical error. Claim 11 has been canceled in view of the incorporation of its limitations in Claim 1. Claim 21 has been amended to further define the structure of the carbon molecular sieve. Support for the amendments to Claim 21 and the limitations of new Claims 28-29 are supported by, for example, the specification from page 3, line 28 to page 4, line 2. Claims 25 and 26 have been amended to delete part of their language that has been incorporated in Claim 21 as amended. As such, the amendments are fully supported by the application as originally filed and do not constitute the addition of new matter. Applicants respectfully request the entry of the amendments.

Foreign Priority Claim and Submission of Priority Document

Applicants have noticed that the claim of foreign priority under 35 U.S.C. § 119 and the submission of certified copy of the priority document are not acknowledged on the summary page of the Office Action. The claim of foreign priority under 35 U.S.C. § 119 based on Korean Patent Application No. 10-2001-0023541 was made in Applicants' Declaration filed on May, 6 2002. A certified copy of the priority document was also submitted on October 25, 2001. Applicants respectfully request that acknowledgement of the priority claim and the receipt of the priority document be made in the next Office Action or communication.

Discussion of Rejection Under 35 U.S.C. §§ 102 and 103

Claims 1-27 have been rejected under 35 U.S.C. §§ 102 and/or 103 based on various references. Applicants have carefully reviewed the Examiner's rejections but respectfully disagree and submit that the presently pending claims are patentable over the references as discussed below.

Claimed Invention

Independent Claim 1 is directed to a process for preparing a carbon molecular sieve. The claimed method recites various steps to produce the carbon molecular sieve. Claim 1 features, among others, that the template comprises SBA-15, Aluminum SBA-15, SBA-3 or Aluminum SBA-3. The claimed method recites the features that carbon atoms in the molecular sieve form nano-lines or nano-tubes arranged in a substantially uniform hexagonal structure.

Independent Claim 21 is directed to a carbon molecular sieve comprising an internal structure of carbon atoms. Claim 21 recites, among other features, that the carbon atoms form nano-lines or nano-tubes arranged in a substantially uniform hexagonal structure.

Discussion of Rejection under 35 U.S.C. § 102(b) Based on Lee

Claims 1-10, 16 and 18-26 have been rejected under 35 U.S.C. § 102(b) as being anticipated by Lee *et al.*, "Synthesis of a New Mesoporous Carbon and Its Application to Electrochemical Double-Layer Capacitors," *Chem. Commun.* 1999, 2177-2178 (hereinafter "Lee"). In response, Applicants note that "[a] claim is anticipated only if each and every element as set forth in the claim is found, either expressly or inherently described, in a single prior art reference." *See, e.g., Verdegaal Bros. v. Union Oil Co. of California*, 814 F.2d 628, 631, 2 USPQ2d 1051, 1053 (Fed. Cir. 1987). Applicants respectfully submit that Lee does not disclose every element of the rejected claims.

Lee discloses preparation of a mezoporous carbon, SNU-1, using the template of a mezoporous aluminosilicate, AlMCM-48, which is an aluminum-implanted form of silica, MCM-48. As noted above, independent Claim 1 recites that the template comprises SBA-15, Aluminum SBA-15, SBA-3 or Aluminum SBA-3. As the Examiner correctly notes in rejecting Claim 11 under 35 U.S.C. § 103(a), Lee does not disclose the materials recited in Claim 1.

Further, both independent Claims 1 and 21 recite that carbon atoms in the molecular sieve

form nano-lines or nano-tubes arranged in a substantially uniform hexagonal structure. Lee does not disclose or teach the recited structure of the carbon molecular sieve. The internal structure of the mezoporous carbon SNU-1 follows the internal structure of the template AlMCM-48 or MCM-48, which is in "cubic Ia3d" structure. *See*, for example, J.C. Vartuli *et al.*, "Effect of Surfactant/Silica Molar Ratios on the Formation of Mesoporous Molecular Sieves: Inorganic Mimicry of Surfactant Liquid-Crystal Phases and Mechanistic Implications," Chem. Mater. Vol. 6, 2317, 1994 (Appendix I), discussion under heading "Cubic MCM-48, X-ray Diffraction" at page 2320. As such, Lee does not disclose or teach a hexagonal structured carbon molecular sieve.

In view of the foregoing, Lee anticipates neither Claim 1 nor Claim 21. Accordingly, Claims 2-10 and 12-29 depending from Claim 1 or 21, not only those rejected, are not anticipated by Lee. Applicants respectfully request withdrawal of the rejection.

Discussion of Rejection Under 35 U.S.C. § 103 Based on Lee and the Present Application

Claim 11 has been rejected under 35 U.S.C. § 103(a) as being unpatentable over Lee alone or in view of Application's specification. Applicants respectfully disagree and submit that Lee alone or in combination with the present specification does not render the presently claimed invention obvious.

The Patent and Trademark Office has the burden under section 103 to establish a prima facie case of obviousness. *In re Piasecki*, 745 F.2d 1468, 1471-72, 223 USPQ 785, 787-87 (Fed. Cir. 1984). To establish a *prima facie* case of obviousness, three basic criteria must be met: first, there must be some suggestion or motivation, either in the references themselves or in the knowledge generally available to one of ordinary skill in the art, to modify the reference or to combine reference teachings; second, there must be a reasonable expectation of success; and finally, the prior art reference (or references when combined) must teach or suggest all the claim limitations. *See* M.P.E.P. § 2143.

Claim 11 has been canceled for the sole purpose of advancing the prosecution. Claim 1 now incorporates the limitations of canceled Claim 11. As discussed above for the anticipation rejection, Claim 1 and Lee differ in that, among other features, Lee does not disclose the recited template materials and further not disclose a substantially uniform hexagonal structure of the carbon nano-lines or nano-tubes.

With regard to the template materials, the Examiner asserts that Applicants appear to admit that they are old and known porous inorganic materials. Applicants acknowledge that the present specification mentions SBA-15 at page 2, lines 2-6 as part of the Description of Related Art. However, Applicants respectfully submit that the statement regarding SBA-15 does not have any bearing on its qualification as prior art and cannot be interpreted as an admission to that effect. As such, Applicants respectfully submit that the present specification cannot be relied on to reject the presently claimed invention. As noted above, Lee does not disclose the recited template materials and further not disclose a substantially uniform hexagonal structure of the carbon nano-lines or nano-tubes. Therefore, Lee cannot establish *prima facie* case of obviousness.

Further, Applicants respectfully submit that even if SBA-15 were in the prior art, its combination with Lee does not disclose a substantially uniform hexagonal structure of the carbon nano-lines or nano-tubes. As such, all of the claimed limitations are not provided by the combination. Moreover, Lee focuses only on MCM-48 and its resulting carbon molecular sieve, SNU-1, and is not concerned with another template. "The teaching or suggestion to make the claimed combination and the reasonable expectation of success must both be found in the prior art, not in applicant's disclosure." *In re Vaeck*, 947 F.2d 488, 20 USPQ2d 1438 (Fed. Cir. 1991). Without reference to the disclosure of the present invention, there no is teaching or suggestion to modify Lee by replacing MCM-48 with SBA-15 to arrive at the claimed invention. For these additional reasons, no *prima facie* obviousness has been established.

In view of the foregoing, Claim 1 is patentable over Lee alone or in combination with qualified statements of prior art, if any, in the present specification. Claims 2-10, 12-20, 28 and 29 depend from Claim 1 and further define the present invention with additional technical features. In view of the patentability of Claim 1 and in further view of the additional technical features, Claims 2-10, 12-20, 28 and 29 are patentable over Lee alone or in combination with qualified statements of prior art, if any, in the present specification.

Discussion of Rejection Under 35 U.S.C. § 103 Based on Lee, Lester and Hucke

Claims 12, 13 and 17 have been rejected under 35 U.S.C. § 103 (a) as being unpatentable over Lee in view of Lester *et al.* (U.S. Patent No. 4,425,316, hereinafter "Lester") or Hucke (U.S. Patent No. 4,329,260). The references in combination or alone do not render the presently claimed

invention obvious as discussed below.

Lester and Hucke are relied on to provide deficiencies of Lee in rejecting Claims 12, 13 and 17. Lester allegedly provides teaching of carbohydrates as a carbon source. Hucke allegedly provides teaching of furfuryl alcohol. However, neither Lester nor Hucke provides the deficiencies of Lee with respect to Claim 1. Particularly, neither the materials for template nor the hexagonal structure of the carbon molecular sieve is provided in Lester or Hucke. Absent such teachings or suggestion, the combination of the cited references do not provide all of the limitations of Claim 1, and no *prima facie* case of obviousness has been established. Therefore, Claim 1 and its dependent claims including Claims 12, 13 and 17 are patentable over the references of Lee, Lester and Hucke.

Discussion of Rejection under 35 U.S.C. § 102(b) Based on Ryoo

Claims 1-6, 8-10, 12-15, 18-26 have been rejected under 35 U.S.C. § 102(b) as being anticipated by Ryoo *et al.*, "Synthesis of Highly Ordered Carbon Molecular Sieves via Template-Mediated Structural Transformation," J. Phys. Chem., Vol. 103, No. 37, 7743-7746 (hereinafter "Ryoo"). Applicants respectfully submit that none of the rejected claims are anticipated by Ryoo as discussed below.

Ryoo discloses preparation of a carbon molecular sieve using MCM-48 as a template. The resulting carbon molecular sieve, CMK-1, has a cubical internal structure, cubic $I4_132$. *See* Ryoo at page 7744, the first paragraph. Ryoo fails to disclose any of the recited template materials, SBA-15, Aluminum SBA-15, SBA-3 or Aluminum SBA-3. Further, Ryoo discloses a carbon molecular sieve having a cubic structure, not a hexagonal structure as recited in Claim 1 and 21. As such, each and every limitation of Claim 1 or 21 is not disclosed in Ryoo. Therefore, Ryoo does not anticipate Claim 1 or 21, nor their dependent claims, Claim 2-10, 12-29.

Discussion of Rejection under 35 U.S.C. § 102(a) Based on Jun

Claims 1-6, 8-10, 12-15, 18-26 have been rejected under 35 U.S.C. § 102(a) as being anticipated by Jun *et al.*, "Synthesis of New, Nanoporous Carbon with Hexagonally Ordered Mesostructure," J. Am. Chem. Soc. 2000, 122 10712 (hereinafter "Jun"). Applicants respectfully submit that Jun does not qualify as prior art under 35 U.S.C. § 102(a) as discussed below.

Jun was published on the Internet on October 12, 2000, as noted at the bottom of its page 10712. Jun was published in paper on November 1, 2002 in Issue 43 of Volume 122 of Journal of

American Chemical Society. The Internet Web Site of Journal of American Chemical Society confirms the November 1, 2002 publication of its Issue 43 of Volume 122, and a copy of the Web Site is attached hereto (Appendix II) listing Jun at page 5. As such, the earliest date of publication of Jun is its online publication on October 12, 2000.

To qualify as prior art under 35 U.S.C. § 102(a), a publication must be published before the invention at issue. As stated in the accompanying Declaration under 37 C.F.R. § 1.131 by the inventors of the claimed invention, actual reduction to practice of the claimed invention was complete prior to October 12, 2000. The publication of Jun was not before the invention of the present application. Therefore, Jun does not qualify as prior art under 35 U.S.C. § 102(a). Applicants respectfully request withdrawal of the rejection.

Discussion of Rejection under 35 U.S.C. § 112

The Examiner has rejected Claims 25 and 26 under 35 U.S.C. § 112, first paragraph, as failing to comply with the written description or enablement requirement. Irrespective to this rejection, some limitations of Claims 25 and 26 have been deleted, but instead incorporated into Claims 1 and 21. Thus, amended Claims 1, 21, 25 and 26 include the limitations of original Claims 25 and 26. Applicants respectfully submit that the present application provides proper written description and enabling disclosure for the subject matter claimed in Claims 1, 21, 25 and 26, as discussed below.

The Examiner asserts that there is no description of how one can make the structure recited in the rejected claims. Applicants respectfully object to the Examiner's assertion and submit that the present specification provides sufficient descriptions of how to make the claimed carbon molecular sieves. Examples 1-7 at pages 7-12 of the present specification describe actual experimentation of making, analyzing and using carbon molecular sieves, CMK-3 and CMK-5, on which the limitations of original Claims 25 and 26 are read. As described in the examples of the specification, both CMK-3 and CMK-5 have a substantially uniform hexagonal structure. CMK-3 has pores generally having a single substantially uniform diameter, while CMK-5 has pores generally having two substantially uniform diameters.

The Examiner also asserts that there is no evidence that the structures recited in Claims 25 and 26 are present, particularly since decomposition of organic material is not recognized as a way to make a carbon nanotube. Applicants respectfully object to the Examiner's assertion and

submit that the specification is not required to provide evidence of the existence of a claimed structure under 35 U.S.C. § 112, first paragraph. Regardless, Figures 1 and 7 show transmission electron micrograms of CMK-3 and CMK-5, which support the existence of the claimed structures. *See also* the present specification at page 7, lines 25-27. Further, Figures 2 and 8 show XRD patterns of CMK-3 and CMK-5, which are interpreted to show a uniform hexagonal structure, as stated at page 7, line 27-29. With regard to the Examiner's assertion that decomposition of organic material is not recognized as a way to make a carbon nanotube, Applicants respectfully submit that the Examiner's non-recognition cannot be a sufficient ground to disregard the ample evidence for the existence of the claimed structure provided in the present application and to question the existence of such a structure. Further, the Lee reference relied on by the Examiner in the rejections under 35 U.S.C. §§ 102 and 103 uses the decomposition of organic material to make a carbon molecular sieve. Absent any evidence contrary to the present disclosure, Applicants respectfully request withdrawal of the rejection.

CONCLUSION

In view of Applicants' amendments to the claims and the foregoing remarks, Applicants respectfully submit that the present application is in condition for allowance. Should the Examiner have any remaining concerns that might prevent the prompt allowance of the application, the Examiner is respectfully invited to contact the undersigned at the telephone number appearing below.

Respectfully submitted,

KNOBBE, MARTENS, OLSON & BEAR, LLP

Dated: 3/1/04

By: _____

Mincheol Kim
Registration No. 51,306
Agent of Record
Customer No. 20,995
(619) 235-8550

S:\DOCS\MCK\MCK-8767.DOC
022704

Appendix I

Chem. Mater. **1994**, *6*, 2317–2326

Effect of Surfactant/Silica Molar Ratios on the Formation of Mesoporous Molecular Sieves: Inorganic Mimicry of Surfactant Liquid-Crystal Phases and Mechanistic Implications

J. C. Vartuli,*,† K. D. Schmitt,† C. T. Kresge,‡ W. J. Roth,‡ M. E. Leonowicz,‡ S. B. McCullen,† S. D. Hellring,† J. S. Beck,† J. L. Schlenker,† D. H. Olson,† and E. W. Sheppard†

Mobil Research and Development Corporation, Central Research Laboratory, Princeton, New Jersey 08543, and Paulsboro Research Laboratory, Paulsboro, New Jersey 08066

Received April 15, 1994. Revised Manuscript Received August 15, 1994[⊗]

The influence of surfactant/silica molar ratio (Sur/Si) in the synthesis of the mesoporous molecular sieve materials (M41S) was studied in a simple ternary synthesis system containing tetraethylorthosilicate (TEOS), water, and the cetyltrimethylammonium (CTMA) cation at 100 °C. The resulting silicate materials were characterized by X-ray diffraction, ^{29}Si NMR, and FTIR. As the Sur/Si molar ratio increased from 0.5 to 2, the siliceous products obtained could be classified into four separate groups: MCM-41 (hexagonal), MCM-48 (cubic), thermally unstable M41S, and a molecular species, the cubic octamer $[(CTMA)SiO_{2.5}]_8$. One of the thermally unstable structures has been identified as a lamellar phase. These results are consistent with known micellar phase transformations that occur at various surfactant concentrations and reinforce the concept that liquid-crystal structures serve as templating agents for the formation of M41S type materials.

Introduction

The discovery of a new family of mesoporous molecular sieves (M41S) was recently reported by researchers at Mobil R&D Corp.[1] and has been the subject of several review articles.[2] M41S materials exhibit narrow pore size distributions, similar to those exhibited by zeolitic materials. However, the pore systems of M41S materials can be tailored with dimensions between 15 and 100 Å. High hydrocarbon sorption capacity and thermal stability are also attractive properties of these new molecular sieves. The M41S family contains several unique members, MCM-41, having a hexagonal arrangement of unidimensional pores, MCM-48, exhibiting cubic structure which can be indexed to an *Ia3d* unit cell, and other species whose structures have not yet been elucidated. M41S materials exist in a wide range of compositions and are synthesized hydrothermally in the presence of alkyltrimethylammonium surfactant cations having an alkyl side chain of greater than six carbon atoms.

As noted in our earlier work, the role of surfactant chemistry is critical for the formation of these materials.[1,3] Surfactant molecules have the ability to assemble into supramolecular arrays that form liquid-crystal structures. A liquid-crystal templating mechanism (LCT) in which surfactant liquid-crystal structures serve as organic templates (rather than single molecules commonly proposed as templates in zeolite synthesis) has been proposed for the formation of these M41S type materials.[1,3] Both the generation of varied pore size MCM-41 by either the use of different length surfactant molecules or by use of micellar solubilization techniques, and the existence of M41S materials having structures (hexagonal, cubic, and lamellar) that mimic known liquid-crystal phases strongly support this proposed mechanism. Two possible mechanistic pathways suggest either (A) the liquid-crystal phase may form prior to the addition of the reagents or (B) the silicate species generated in the reaction mixture may influence the ordering of surfactant micelles to the desired liquid crystal phase.[1,3]

For either pathway, the resultant composition would produce an inorganic material that mimics known liquid-crystal phases. For pathway A to be operative, it is required that the surfactant molecules exist in sufficient concentration for a liquid-crystal structure to form. This liquid-crystal structure serves as the templating agent and the inorganic silicate anions merely serve to counterbalance the charge of these fully ordered surfactant aggregates. For pathway B, surfactant is only part of the template. The presence of a silicate anion species not only serves to charge balance the surfactant cations but also participates in the formation and ordering of the liquid-crystal phase.

Surfactant literature data do not support pathway A, especially for the alkyltrimethylammonium cation system, since the presence of the various liquid-crystal structures appears unlikely at the concentrations used

† Mobil Research and Development Corp., Central Research Laboratory.

‡ Mobil Research and Development Corp., Paulsboro Research Laboratory.

⊗ Abstract published in *Advance ACS Abstracts,* November 1, 1994.

(1) Kresge, C. T.; Leonowicz, M. E.; Roth, W. J.; Vartuli, J. C.; Beck, J. S. *Nature* **1992**, *359*, 710–712.

(2) Ozin, G. A. *Adv. Mater.* **1992**, *4* (10), 612–48. Behrens, P. *Adv. Mater.* **1993**, *5* (2), 127–32. Behrens, P.; Stucky, G. D. *Angew. Chem., Int. Ed. Engl.* **1993**, *32* (5), 696–99. Davis, M. E. *Nature* **1993**, *364*, 391–93.

(3) Beck, J. S.; Vartuli, J. C.; Roth, W. J.; Leonowicz, M. E.; Kresge, C. T.; Schmitt, K. D.; Chu, C. T.-W.; Olson, D. H.; Sheppard, E. W.; McCullen, S. B.; Higgins, J. B.; Schlenker, J. L. *J. Am. Chem. Soc.* **1992**, *114* (27), 10834–43.

0897-4756/94/2806-2317$04.50/0

to form M41S structures.[4] The synthesis data presented herein show that hexagonal, cubic, and lamellar M41S structures form by varying the silica concentration at constant surfactant concentration, thus implicating a more prominent role for the inorganic silicate anions.[3] It is these synthetic data that support pathway B and are the subject of this article.

Experimental Section

Materials. Tetraethylorthosilicate (TEOS), trimethylsilyl chloride, and hexamethyldisiloxane were obtained from Aldrich. Cetyltrimethylammonium chloride ($C_{16}H_{33}(CH_3)_3NCl$), 29 wt % aqueous solution, was obtained from Armak Chemicals. The $C_{16}H_{33}(CH_3)_3N^+OH/Cl^-$ solution was prepared by batch exchange of the 29% $C_{16}H_{33}(CH_3)_3NCl$ with IRA-400(OH) exchange resin, Rohm and Haas. The effective exchange of hydroxide for halide was ~30%. All chemicals were used as received.

Instrumentation. X-ray powder diffraction was obtained on a Scintag XDS 2000 diffractometer using Cu Kα radiation of wavelength 1.541 78 Å, a step size of 0.04° 2θ, a counting time per step of 10–100 s, and an energy-dispersive detector. Peak positions and peak amplitudes were obtained using a deconvolution algorithm supplied by Scintag. High-resolution transmission electron microscopy (TEM) images and electron diffraction patterns of microtomed sections were obtained on a JEOL 200 CX. Images from thin sections and thin grain edges were recorded under various focus conditions. Diffraction information from M41S materials is limited to relatively large *d* spacings, and the diffracted intensities are weak. Images show contrast reversal upon going through Gaussian focus, as expected from the appearance of the electron diffraction pattern. Furthermore, no reversal in image contrast is observed at large under focus conditions. These characteristics suggest that a weak phase object approximation is reasonable for the interpretation of these images. According to this interpretation, the light areas in the images correspond to a lack of scattering matter (pores), and the dark areas are concentrations of scattering matter (walls).

Benzene sorption data were obtained on a computer-controlled 990/951 DuPont TGA system. The calcined sample was dehydrated by heating at 350 or 500 °C to constant weight in flowing He. Benzene sorption isotherms were measured at 25 °C by blending a benzene saturated He gas stream with a pure He gas stream in the proper proportions to obtain the desired benzene partial pressure. Argon physisorption measurements were conducted on a physisorption apparatus as previously described.[5] The method of Horváth and Kawazoe[6] was used to determine pore diameters.

Si NMR spectra were obtained on a JEOL Tecmag 200 MHz NMR in 9.5 mm zirconia rotors at 39.64 MHz spinning 4–4.2 kHz using 90° pulses at 1200 s intervals with high-power proton decoupling. Between 36 and 72 pulses gave high-quality spectra. Air was used as the drive gas to obtain as much benefit as possible from O_2 paramagnetic relaxation.[7] TMS (tetramethylsilane) was used as shift standard.

Infrared spectral data were gathered using a Nicolet 7199 under a N_2 purge at 4 cm^{-1} resolution with an MCT-B detector. The samples were ground in KBr or polyethylene and pressed into thin wafers prior to analysis.

Synthesis. Tetraethylorthosilicate (TEOS) and the $C_{16}H_{33}(CH_3)_3N^+OH/Cl^-$ solution were combined in various proportions to give the appropriate surfactant to silica molar ratio (designated as Sur/Si ratio). No additional water was added to the syntheses. The two reactants were mixed for 1 h to allow the hydrolysis of the TEOS. In separate sets of experiments this hydrolysis step was conducted at both room temperature (~25 °C) and at ~4 °C. When the hydrolysis of the TEOS was conducted at ~4 °C, the products were similar to those obtained from the room-temperature hydrolysis experiments, but phase transformations took place at higher Sur/Si ratios. For example, the cubic structure was observed at ratios as high as 1.5 when the hydrolysis was conducted at 4 °C compared to approximately 1.0 for ambient temperature hydrolysis. The reasons for this effect are not apparent at this time, although it may be due to the variation in the concentration of silicate species as a function of the hydrolysis temperature. These mixtures were placed in polypropylene bottles and placed into a steam box (~100 °C) for 48 h. The caps of the polypropylene bottles containing the reactant mixtures were deliberately left loosely fastened in the steambox to allow for the evaporation of the ethanol produced in the hydrolysis of the TEOS. Any variation of product was attributed to the change in the surfactant/silica ratio. This ratio was varied between 0.5 and 2.

Table 1. Composition of Synthetic Mixtures for the Formation of Various M41S Phases

product	Sur/Si	TEOS/100 g of CTMAOH
MCM-41	0.6	30 g
MCM-48	1.0	20 g
lamellar	1.3	15 g
cubic octamer	1.9	10 g

The amounts of TEOS and CTMAOH solution used to synthesize examples of these four main groups of materials are shown in Table 1. The resultant products were recovered by filtration, washed in water, and air-dried at ambient temperature. The as-synthesized products were then calcined at 540 °C for 1 h in flowing nitrogen followed by 6 h in flowing air.

As the Sur/Si molar ratio was varied, the products formed could be grouped into four main categories: Sur/Si < 1 hexagonal (MCM-41), Sur/Si = 1–1.5, cubic (MCM-48), Sur/Si = 1.2–2, thermally unstable materials, and finally Sur/Si = 2 the cubic octamer, $[(CTMA)SiO_{2.5}]_8$, is formed. The thermally unstable materials produce fairly well-defined X-ray diffraction (XRD) patterns in the as-synthesized form but upon calcination lost most, if not all, XRD definition. One of these thermally unstable species exhibited an XRD pattern consistent with a lamellar type structure (a common liquid-crystal phase).

The X-ray diffraction pattern of the as-synthesized MCM-41 material exhibited a high-intensity peak having a *d* spacing of approximately 40 Å and several higher angle peaks having *d* spacings consistent with hexagonal indexing of *kk*0 reflections. X-ray diffraction of the calcined MCM-41 revealed a high intensity first peak having a *d* spacing of approximately 34 Å (representing a lattice contraction after calcination of about 5 Å, $(6 \times \sqrt{3})/2$) and other peaks consistent with hexagonal *hk*0 indexing. The lattice contraction for MCM-41 materials varied depending on synthesis conditions. The X-ray diffraction pattern of the calcined material is shown in Figure 1a. Found in the as-synthesized product (wt %): C, 47.5; N, 2.29; Si, 15.3; ash (1000 °C), 32.0.

The X-ray diffraction pattern of the as-synthesized MCM-48 exhibited a high-intensity peak having a *d* spacing of approximately 39 Å and several higher angle peaks having *d* spacings consistent with cubic indexing. X-ray diffraction pattern of the calcined version revealed a high intensity first peak having a *d* spacing of approximately 33 Å (representing a lattice contraction after calcination of about 14 Å) and several peaks having *d* spacings with retention of the cubic indexing. The X-ray diffraction pattern of the calcined product is shown in Figure 1b. Found in the as-synthesized product (wt %): C, 33.4; N, 1.88; Si, 11.7; ash (1000 °C), 25.9.

The X-ray diffraction pattern of the as-synthesized lamellar material exhibited a high intensity peak having *d* spacings of approximately 36 Å and two higher angle peaks having *d* spacings (18 and 12 Å) consistent with lamellar indexing of

(4) Reiss-Husson, F.; Luzzati, V. *J. Phys. Chem.* **1964**, *68* (12), 3504–11.
(5) Borghard, W. S.; Sheppard, E. W.; Schoennagel, H. J. *Rev. Sci. Instrum.* **1991**, *62*, 2801–2809.
(6) Horváth, G.; Kawazoe, K. J. *Chem. Eng. Jpn.* **1983**, *16* (6), 470–475.
(7) Cookson, D. J.; Smith, B. E. *J. Magn. Reson.* **1985**, *63*, 217–218. Klinowski, J.; Carpenter, T. A.; Thomas, J. M. *J. Chem. Soc., Chem. Commun.* **1986**, 956–958.

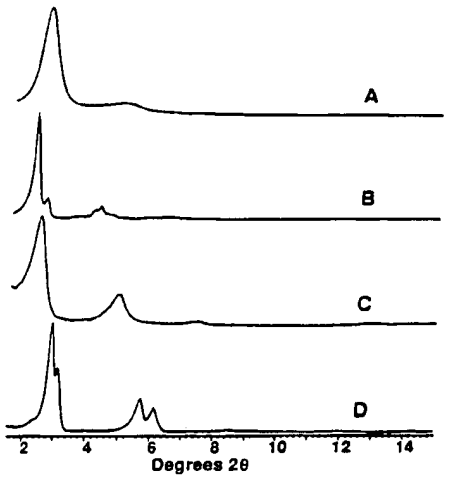

Figure 1. X-ray diffraction patterns of (A) calcined MCM-41, (B) calcined MCM-48, (C) as-synthesized lamellar material, and (D) cubic octamer.

00*l* reflections as shown in Figure 1c. Upon calcination at 540 °C the X-ray diffraction pattern was featureless. Found in the as-synthesized product (wt %): C, 45.1; N, 2.24; Si, 14.4; ash (1000 °C), 30.8.

The X-ray diffraction pattern of the as-synthesized cubic octamer material is shown in Figure 1d. After calcination at 540 °C, the X-ray diffraction pattern was featureless indicating that this material is unstable to this thermal treatment. Found in the as-synthesized product (wt %): C, 53.8; N, 2.76; Si, 6.8; ash (1000 °C), 14.2.

As is the case for the synthesis of MCM-41, MCM-48 and the lamellar material can be prepared from various alkyltrimethylammonium cations systems and under a variety of synthetic conditions. These factors will affect both the pore size of the product and the relative location of the peaks in the XRD pattern.

Trimethylsilylation. In a typical experiment, 0.50 g of sample, 10 g of trimethylsilyl chloride (TMSCl), and 15 g of hexamethyldisiloxane (HMDS) were refluxed overnight with magnetic stirring under N_2. The volatiles were stripped on a rotary evaporator, and the dry powder was washed two or three times with 10 mL of reagent grade acetone with centrifuging. Material recovery was typically >98%.

The trimethylsilylated silicate octamer, Q8M8, was prepared by adding, in order, 200 mL of DMF, 100 mL of HMDS, and 50 mL of TMSCl to 10 g of the organic silicate octamer in an Erlenmeyer flask and stirring magnetically for 20 min. The mixture was diluted with 200 mL of pentane, 100 mL of H_2O was added, the layers were separated, the organic was washed with another 50 mL of H_2O, the organic was stripped, the solid was taken up into 200 mL of cyclohexane, filtered and the product crystallized by slow evaporation of the solvent to give 3.16 g (97% yield) of waxy, white solid.

Results and Discussion

The X-ray diffraction and NMR data were used to establish the presence of four primary synthetic products. We first describe the general NMR data, then address in further detail the characterization of the individual materials, and finally discuss how these results support a silicate-initiated mechanistic pathway.

General NMR Data. Solid-state MAS Si NMR of the four primary as-synthesized materials is summarized in Figure 2 and Table 2. The spectra could be sorted into those with three overlapping broad peaks (hexagonal or cubic phases), two peaks (lamellar), and one peak (the cubic octamer). MCM-41 and MCM-48 have essentially the same ^{29}Si NMR spectra as amorphous silica. They show three broad peaks from Q4, Q3, and Q2 silicons (framework, silanol, disilanol). The peaks are broad, reflecting a wide range of Si–O–Si bond angles. The shifts and intensities were obtained by deconvolution.

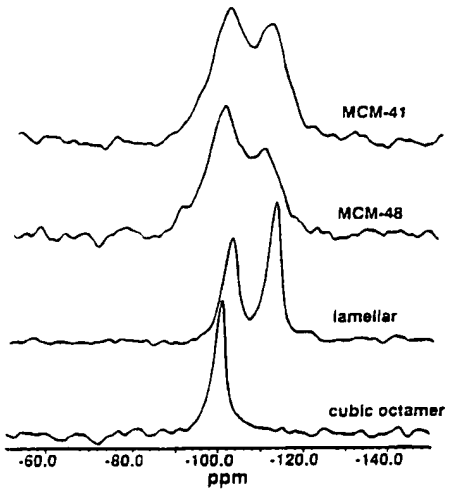

Figure 2. ^{29}Si NMR data of various Sur/Si products: (A) calcined MCM-41 (B), calcined MCM-48, (C) as-synthesized lamellar material, and (D) cubic octamer.

Table 2. ^{29}Si NMR Data for As-Synthesized Products

	chemical shift			mole %		
type	Q2	Q3	Q4	Q2	Q3	Q4
MCM-41	−89.1	−98.2	−108.0	8	49	43
MCM-48	−89.1	−98.2	−108.0	8	54	38
lamellar		−101.0	−111.1		52	48
octamer		−99.8			100	

In this synthesis system, as the Sur/Si increases, Q3 remains about the same (~50%) from MCM-41, MCM-48, and the lamellar material and increases to 100 mol % for the octamer. However, the Q3 content can vary depending on the synthesis conditions. The chemical analyses of the as-synthesized products are consistent with the invarient Q3 content. The N/Si molar ratio (initially assumed to represent the Q3 content) shows no variation with changes in the Sur/Si charge for the MCM-41, MCM-48, and lamellar products. Except for the octamer, the N/Si ratio remains unchanged at ~0.30. For the octamer, the N/Si ratio was 0.81 where the expected value should be 1.00. The lack of agreement in the absolute numbers, Q3 (50%) and the N/Si ratios (30%), may indicate that some of the Q3 are not associated with the surfactant and may represent silanols or silanol nests formed in areas of incomplete silica condensation.

Characterization of the Individual Synthesized Materials

Hexagonal MCM-41. MCM-41 has been characterized previously.[3] Generally, MCM-41 exhibits an XRD pattern containing three or more low-angle peaks that can be indexed to a hexagonal *hk*0 pattern. MCM-41 characteristically exhibits a hydrocarbon sorption capacity of 0.7 mL/g or greater and the sorption isotherm contains a sharp inflection at a p/p_0, dependent on the pore size of the MCM-41, suggesting a uniform size pore system. Argon physisorption data confirm this narrow

Table 3. X-ray Diffraction Peaks and Cell-Parameter Refinement for Calcined Cubic MCM-48[a]

peak	index	2Θ	calculated 2θ	Δ2θ	rel intensity
1	211	2.670	2.669	0.001	100.0
2	220	3.085	3.081	0.004	12.3
3	321	4.066	4.077	−0.011	1.2
4	400	4.353	4.358	−0.005	1.1
5	420	4.874	4.873	0.001	3.8
6	332	5.109	5.111	−0.002	6.0
7	422	5.349	5.338	0.001	2.3
8	431	5.560	5.557	0.003	1.6

[a] a_0 (unit cell) = 81.09 (5) Å. (The quantity in parentheses is an estimated standard deviation (esd). This parameter is a measure of precision, not accuracy.)

pore size distribution. Depending on synthetic conditions, MCM-41 can be prepared with pore sizes ranging from ~15 to 100 Å.

Cubic MCM-48. X-ray Diffraction. A total of eight peaks were used to index the X-ray diffraction pattern of the calcined sample. The data and the results of this refinement in which all eight of the observed reflections were accounted for are shown in Table 3.

Comparison of the *d* spacings observed in this refinement yields a good correspondence to those predicted by the cubic *Ia3d* phase known in the surfactant literature. The calculated unit cell parameters, ~80 Å for the calcined MCM-48 sample were somewhat smaller than those observed, ~99 Å, for the cetyltrimethylammonium bromide "oil in water" *Ia3d* cubic analog.[8] However, this difference may reflect the shrinkage of the unit cell upon calcination due to further condensation of the silicate lattice. The cell parameter agreement is better for the as-synthesized MCM-48 material having an ~95 Å unit cell. A more systematic approach was applied to indexing the X-ray powder diffraction pattern of calcined MCM-48 preparation using a procedure developed by Bloss.[9] This procedure is applicable only to crystals belonging to the cubic crystal system. It was found that the XRD powder pattern of calcined MCM-48 could be indexed completely on the basis of a unit cell with $a = 81.09$ (5) Å. The observed reflections (Table 2) suggest systematic absences consistent with the uniquely determinable space group *Ia3d* ($I = h + k + l$, for *hkl*; and with *h,k,l* permutable *k*, (l) = $2n$ for $0kl$ and $2h + l = 4n$ and ($l = 2n$) for *hhl*).[10,11] This assignment also matches crystallographic work on cubic lytropic crystal phases.

Argon Physisorption. Argon physisorption isotherms (Figure 3) were obtained over $0-0.9p/p_0$ using an in-house physisorption apparatus.[5] The pore size of MCM-48, determined by the Horváth–Kawazoe method, was 28 Å (Figure 4). The pore volume was calculated to be approximately 0.60 cm^3/g similar to that obtained from MCM-41 samples having similar pore sizes.

Benzene Sorption. The benzene sorption isotherm of MCM-48 is shown in Figure 5. The isotherm exhibits a sharp inflection characteristic of capillary condensation within uniform pores, where the p/p_0 position of the inflection point is related to the diameter of the pore.[12,13] These characteristics were noted for MCM-41.[3] The p/p_0 of the inflection point for the MCM-48 sample is essentially the same as that for a MCM-41 sample prepared using the dodecyltrimethylammonium cation/TEOS system. These data are consistent with the pore size determination results by argon physisorption reported above.

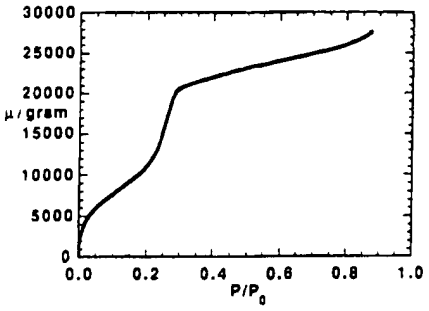

Figure 3. Argon physisorption isotherm of calcined MCM-48.

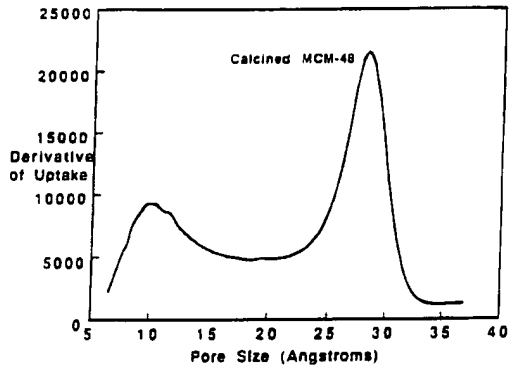

Figure 4. Horváth–Kawazoe argon physisorption plot of calcined MCM-48.

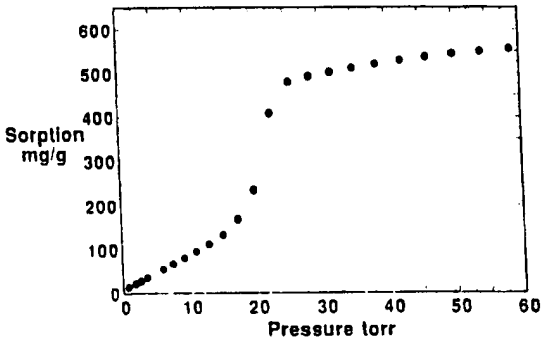

Figure 5. Benzene sorption data of calcined MCM-48.

Transmission Electron Microscopy. Transmission electron micrographs of thin sections of calcined MCM-48 (Figure 6) contain roughly circular regions that are about 1000–2000 Å in diameter. They usually display regular lattice fringes. A variety of two-dimensional lattice fringe patterns is observed in these micrographs, while samples of MCM-41 usually only give its characteristic hexagonal fringe pattern in

(8) Fontell, K. *Colloid Polym. Sci.* **1990**, *268*, 264–285.
(9) Bloss, F. D. *Crystallography and Crystal Chemistry*; Holt, Rinehart, and Winston: New York, 1971; pp 480–482.
(10) *International Tables for Crystallography*; Theo Hahn, Ed.; D. Reidel Publishing Co.: Dordrecht, Holland, 1983; Vol. A, Space-Group Symmetry, p 47.
(11) In ref. 10, p 706.
(12) Gregg, S. J.; Sing, K. S. W. *Adsorption, Surface Area, and Porosity*, 2nd ed.; Academic Press, Inc.: New York, 1982.
(13) Kerr, G. T.; Chester, A. W. *Thermochim. Acta* **1971**, *3*, 113–124.

Figure 6. Transmission electron micrographs of MCM-48.

selected parts of the specimen that happen to be correctly aligned in the *hk*0 projection. The frequency and diversity of fringe patterns suggest that MCM-48 possesses observable three-dimensional order in more than one projection as expected for an analog of the cubic *Ia*3*d* liquid-crystal phase. One particularly interesting image is identified in Figure 6b as feature A. This unique pattern is believed to be the [111] projection of MCM-48.

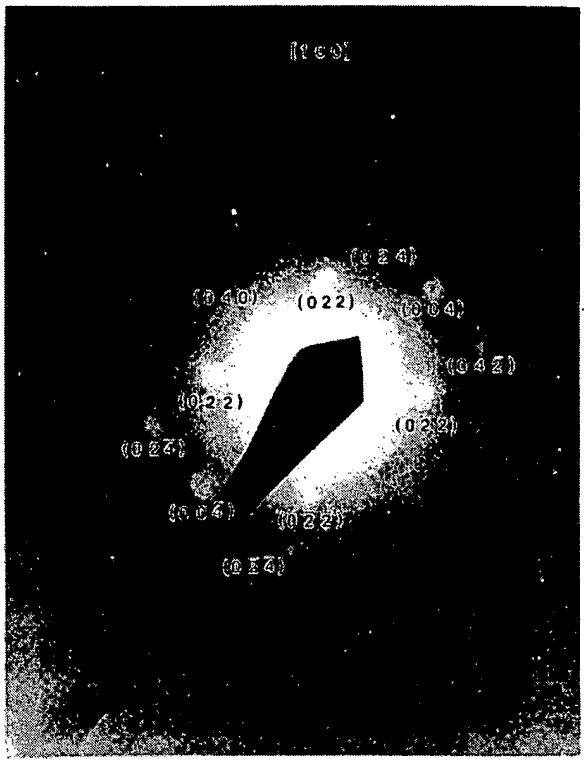

Figure 7. Indexed electron diffraction pattern of MCM-48 showing the [100] projection.

Figure 7 shows an indexed electron diffraction pattern of MCM-48. As expected, the pattern contains only a few diffraction maxima at large *d* spacings. Furthermore, the pattern contains some extraneous spots, indicating that more than one individual crystallite contributed to the electron diffraction pattern. It is reasonable to expect multiple crystal electron diffraction patterns from materials with such small crystal morphologies. Nevertheless, this pattern can be satisfactorily indexed (see Figure 7) as the [100] projection of the cubic *Ia*3*d* phase.

NMR and Silylation Results. The Si NMR spectra in both the as-synthesized and calcined forms of MCM-48 are unexceptional, showing a single broad peak centered at about −110 ppm. The spectra are not substantially different from those of MCM-41 or amorphous silicas. The Si NMR of trimethylsilyl derivatives from both the as-synthesized and calcined forms show narrowing due to conversion of the silanol in Q3 silicons to Q4 silicons by the trimethylsilyl chloride and the appearance of Me_3SiO peak(s) at 14 ppm. Integration showed roughly 16% of the silicons to be silanols in the as-synthesized form. This concentration is 0.67 mequiv/g, roughly half the 1.34 (N analysis)−1.46 mequiv/g (C analysis) of the template. This ratio was one-to-one for MCM-41. Whether this result is due to condensation of some silanols during synthesis or incomplete derivatization by trimethylsilyl chloride is unknown.

Silylation studies of both as-synthesized and calcined forms of MCM-48 produced rather surprising results. The treatment of the as-synthesized MCM-48 with TMSCl resulted in removal of the organic component

Table 4. Argon Physisorption Data for MCM-48 and the Silylated Products

sample	unit cell, Å	argon physisorption data	
		pore diam, Å	pore vol, mL/g
MCM-48 (as synthesized)	95		
organic extracted/silylated[a]	92	34	0.451
organic extracted/silylated[a]	92	34	0.405
MCM-48 (calcined)	81	28	0.608
calcined/silylated	80	26	0.591

[a] Replicate argon physisorption determinations.

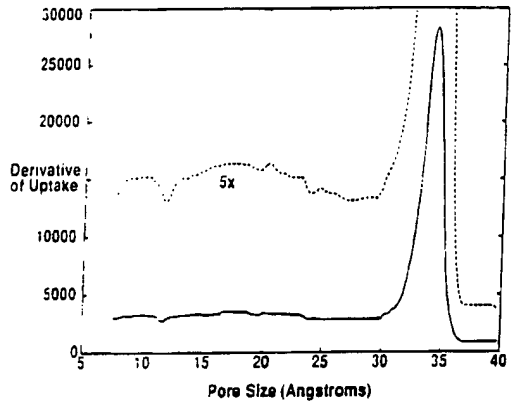

Figure 8. Horváth–Kawazoe argon physisorption plot of silylated MCM-48 from the as-synthesized form.

yielding a porous material with an average pore dimension of 34 Å (Table 4). This was accompanied by a moderate unit cell contraction of about 3 Å. In comparison, removal of the organic by calcination produced a unit-cell contraction of approximately 14 Å and a resultant pore size of about 28 Å. It would appear that the silylation of the silanol groups of MCM-48 (in the as-synthesized form) retarded this unit-cell contraction by removing available sites for silicate condensation. However, in view of the above trend it is difficult to explain why the silylated MCM-48 material with pore openings of 34 Å has a smaller void volume (~0.40–0.45 mL/g) than the 28 Å pore calcined material (~0.6 mL/g).

Figure 8 shows that the argon physisorption of the TMS-treated as-synthesized MCM-48 is unlike any large pore material examined thus far in that it shows no detectable monolayer sorption. The absence of the monolayer sorption peak is puzzling since no TMS-treated MCM-41 showed any such anomalous behavior. The TMS-treated MCM-41 samples showed the 9–10 Å monolayer peak and a decrease in pore volume that correlated quantitatively with the decrease in Horváth–Kawazoe pore diameter.[3]

The silylation of calcined MCM-48 produced only minimal changes in both pore size (from 28 to 26 Å) and void volume (from 0.61 to 0.59 mL/g). This final pore volume, however, is substantially more than that expected (~0.50 mL/g) if silylation reduced the pore diameter as noted for MCM-41 type materials.[3] Figure 9 shows the argon physisorption results for calcined MCM-48 sample and its TMS derivative with the x axis in the Horváth–Kawazoe transform. As expected, the results from the two samples illustrated in Figure 9 show the monolayer peak at 9–10 Å and the pore filling peak at 26 and 28 Å. The monolayer coverage accounts for about 24% of the total pore volume.

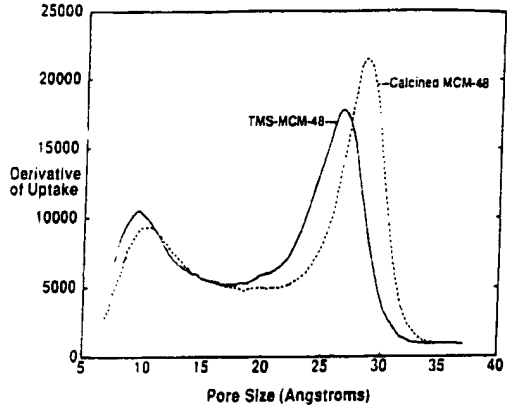

Figure 9. Horváth–Kawazoe argon physisorption plots of calcined MCM-48 and the silylated calcined version.

Structure Considerations. It has been proposed that the individual pores of MCM-41 are obtained from separate cylindrical micelles, while the ordered porous structure results from the hexagonal arrangement of this micellar array.[1,3] The structure of MCM-48 presents a significantly more complex problem than in the case of hexagonal MCM-41. The structure for MCM-48 is expected to be analogous to that of a liquid crystal with the cubic *Ia3d* symmetry, which has not been unequivocally elucidated. Over the years several models for the liquid crystal phase have been put forward. The proposed liquid-crystal structures include compositions with various orderings of (1) spherical, (2) cylindrical shaped micelles, or (3) a more complex system based on a bilayer aggregate that forms an infinite periodic minimal surface.[8,14–18] All three model systems can be indexed on a body-centered cubic lattice. The surfactant aggregate that forms the basis of the packed spherical model is a micellar sphere. For cylindrical ordering models, the cylindrical micelle is the basic unit. The infinite periodic minimal surface structure model uses bilayers of surfactant molecules, as shown in Figure 10. MCM-48 materials corresponding to any of the three proposed liquid-crystal structure models could contain a multidimensional pore system. A liquid-crystal template consisting of ordered spherical micelles forming MCM-48 could be easily visualized (Figure 10). For discrete surfactant micelles, the hydrophilic ends of the surfactant molecule make up the outer surface of the sphere, while the hydrophobic part of the surfactant molecule resides in the inside. A cubic packing of spherical micelles can be used to produce an inorganic structure (after removal of the surfactant molecules) with a three-dimensional pore system similar to that of zeolite A, for example. However, the aggregation of micellar spheres for the formation of the cubic structure has been generally discounted.[19]

The sequence of phases in a phase diagram precludes neither cylindrical micelles nor surfactant bilayers from consideration as the building units for the cubic phase

(14) Fontell, K. *J. Colloid Interface Sci.* **1972**, *43* (1), 156–164.
(15) Tiddy, G. J. T. *Phys. Rep.* **1980**, *57* (1), 1–46.
(16) Ekwall, P.; Mandell, L.; Fontell, K. *J. Colloid Interface Sci.* **1969**, *29* (4), 639–646.
(17) Larsson, L. *J. Phys. Chem.* **1989**, *93*, 7304–14.
(18) Charvolin, J.; Sadoc, J. F. *Colloid Polym. Sci.* **1990**, *268*, 190–95.
(19) Luzzati, V.; Spegt, P. A. *Nature* **1967**, *215*, 701–804.

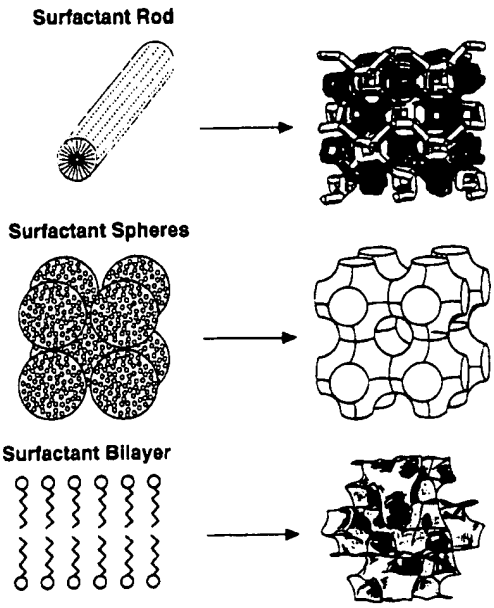

Figure 10. Possible surfactant micellar structures for the MCM-48 template.

since a phase transformation from hexagonal to cubic symmetry using cylindrical micelles is as conceivable as a transformation from the lamellar to cubic symmetry using a surfactant bilayer. The model which is currently most widely cited is a bicontinuous structure that has evolved from the proposal made by Luzzati.[20] The original simplified representation of the structure invoked two infinite three-dimensional, mutually intertwined, unconnected networks of rods made up by one of the components (either amphiphile or solvent). The other component occupied the space in between. The more sophisticated and apparently more realistic representation of this model is based on the concept of infinite periodic minimal surfaces. However, this interpretation is not shared by all the researchers in this field. Fontell differentiates between these two structures and assigns them to different *Ia3d* systems.[21] This controversy seems to indicate that the differences between the two structures are subtle and the problem may not be easily resolved. Additional experimental data that supports a bicontinuous structure for MCM-48 come from two sources: NMR data on the diffusion of water within the liquid-crystal phase[22,23] and the synthesis of a hydrocarbon polymer in the oil part of the cubic phase.[24] Fontell studied the diffusion coefficients of water, hydrocarbon, and surfactant in the systems didodecyldimethylammonium bromide/hydrocarbon/water[22] and monoglyceride/water.[23] He determined that the diffusion coefficients of water, hydrocarbon, and surfactant in the cubic phase were approximately the same as those in the lamellar phase and concluded that the micelle aggregate of the cubic and lamellar phase was the same.

A recent European patent application[24] claims the formation of a hydrocarbon polymer based porous material using the cubic phase of the didodecyldimethylammonium bromide/decane/water system as a template. The polymer product was indexed on a *Ia3d* lattice. This material presumably was formed within the hydrocarbon portion (oil phase) of the liquid-crystal phase, where MCM-48 is formed within the solvent portion (water phase). The ability to form equivalent *Ia3d* porous solids by polymerization in either the oil or water parts of the cubic liquid-crystal phase implies a bicontinuous structure.

A proposed bicontinuous structure for MCM-48 is consistent with the recent work of Monnier et al.[25] They were able to index the XRD pattern of MCM-48 to that predicted for the gyroid form of an infinite periodic minimal surface model (Q^{230}) proposed by Mariani.[26]

Lamellar Phase. The identities of all of the unstable phases formed at Sur/Si of ~1.2–1.8 are not easily elucidated. The unstable phase described above has a characteristic XRD pattern (of the as-synthesized product) of well defined peaks (two or more) that are orders of the initial peak, suggesting some sort of ordered or layered material. This material was unstable when calcined. Lamellar products in surfactant containing syntheses have been suggested.

The unstable TEOS-based lamellar phase may not have thermal stability but it does appear to have crystalline structure. It shows two relatively sharp peaks for Q4 and Q3 silicons in 1:1 ratio in its Si NMR spectrum. The sharpness of these peaks suggests a repeating structure. On removal of template by calcination both the XRD and NMR fine structure disappear, but this is not the case for the silylated version. On treatment of as-synthesized material with TMSCl in HMDS/DMF, 33% of the solid (ash = 64% by TGA) was recovered as a water soluble salt. This material is CTMACl as identified by its C NMR spectrum. The remaining 60% had a Si NMR virtually unchanged from the as-synthesized material, that is, two sharp peaks at −100.9 and −110.5 ppm in 1:1 ratio. The structure was not affected by this treatment, nor was more than trivial trimethylsilylation accomplished. The NMR spectra of magadiite, a known layered silicate (Figure 11) are similar. The only difference is that the percentage of Q3 is higher for the surfactant–TEOS lamellar phase. For magadiite the Q3:Q4 ratio is approximately 35:65, whereas the TEOS lamellar product has a ratio of approximately 50:50 (by peak area). The synthesis temperature for magadiite (~175 °C) is higher than that of the TEOS-based lamellar material (100 °C). The higher Q3 content of the TEOS-based product indicates less polymerization of the silicon network. The broadness of the Q3 and Q4 peaks of the surfactant-based lamellar products relative to that of magadiite also suggests less regularity of the silicon structure.

The lamellar phase could be represented by sheets or bilayers of surfactant molecules with the hydrophilic ends pointed toward the oil–water interface, while the

(20) Luzzati, V.; Tardieu, A.; Gulik-Krzywicki, T.; Rivas, E.; Reiss-Husson, F. *Nature* **1968**, *220*, 485–88.
(21) Fontell, K. *Adv. Colloid Interface Sci.* **1992**, *41*, 127–47.
(22) Fontell, K.; Jansson, M. *Prog. Colloid Polym. Sci.* **1988**, *76*, 169–75.
(23) Lindblom, G.; Larsson, K.; Johansson, L.; Fontell, K.; Forsen, S. *J. Am. Chem. Soc.* **1979**, *101* (9), 5465–70.
(24) Anderson, D. European Patent Application, WO 90/07575, July 12, 1990.
(25) Monnier, A.; Schüth, F.; Huo, Q.; Kumar, D.; Margolese, D.; Maxwell, R. S.; Stucky, G. D.; Kishnamurthy, M.; Petroff, P.; Firouzi, A.; Janicke, M.; Chmelka, B. F. *Science* **1993**, *261*, 1299–1303.
(26) Mariani, P.; Luzzati, V.; Delacroix, H. *J. Mol. Biol.* **1988**, *204*, 165–89.
(27) Sprung, R.; Davis, M. E.; Kauffman, J. S.; Dybowski, C. *Ind. Eng. Chem. Res.* **1990**, *29*, 213–20.

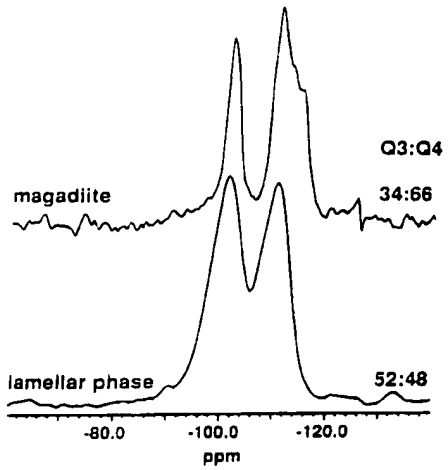

Figure 11. ^{29}Si NMR of (A) magadiite and (B) CTMA lamellar product.

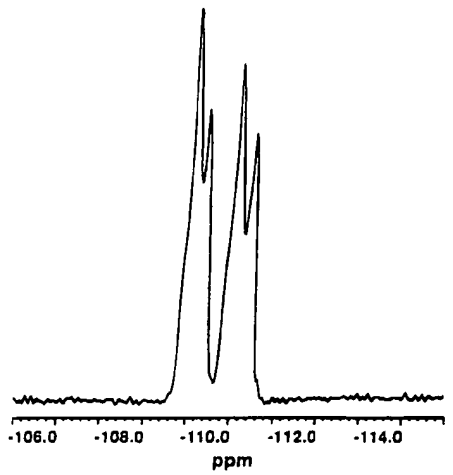

Figure 12. ^{29}Si NMR of Q8M8 product from cubic octamer.

hydrophobic ends of the surfactant molecules face one another. Any silicate structure produced from this liquid-crystal phase would be similar to that of two dimensional layered materials such as magadiite or kenyaite. However, the lack of any observable peaks in the XRD pattern of the lamellar material in the region of 20−25° 2θ suggests that these silicate layers of this lamellar phase are not as well ordered as those of layered silicates. This lack of order may be due to the higher concentration of silanol groups resulting in less condensation of the silicate species as suggested by the NMR data. Removal of the surfactant from between the silicate sheets could result in a condensation of the layers, collapsing any structure and forming a dense phase with little structural order or porosity.

Cubic Octamer. Stabilized silicate octamers have been prepared using other quaternary ammonium compounds.[28-38] They have been characterized by IR,[28] Raman,[29] X-ray diffraction,[30] and NMR.[31,32] All these materials share a double four ring (D4R), $Si_8O_{20}^{8-}$, with the quaternary ions functioning to stabilize the structure. There has been speculation that these double four-ring, D4R, silicate structures are precursors or secondary building units, SBU, for the formation of zeolites.[33-38] However, their hydrothermal stability is poor. For example, the tetramethylammonium cubic octamer is unstable above about 80 °C,[28,34,35] suggesting it is probably not an intermediate in the formation of crystalline materials synthesized at temperatures >100 °C and at relatively high concentrations of alkali metal ions.[39] Because milder synthetic conditions are required for the formation of M41S materials, the cetyltrimethylammonium octamer version could be an intermediate in the formation of these mesoporous molecular sieves. Figure 1d illustrates the X-ray diffraction pattern of the octamer formed in the CTMA system.

Elemental analysis agrees reasonably well with a hydrate with 4.5 H_2O associated with each CTMA. This is consistent with literature results for other tetraalkylammonium D4R species. The tetramethylammonium compound, for example, crystallizes with 8.6 H_2O/TMA.[33]

The trimethylsilylated derivative, referred to in the literature as "Q8M8", was identified on the basis of its solution Si NMR shift and its distinctive five-line solid-state Si NMR spectrum[33] (12.08, −109.12, −109.36, −110.10, and −110.47 ppm), Figure 12. The multiple Q4 peaks arise from crystallographic splitting of the otherwise identical silicons. The crystal is triclinic.[33]

A hydrothermal stability kinetic study was carried out in an NMR tube in situ at 99.8 °C in the NMR probe in parallel with steambox experiments. In agreement with literature observations, most notably the detailed studies of Knight,[31] there is slight evidence for a D4R species in the early stages and none after 24 h. The CTMA silicate octamer is stable indefinitely, in dry form or in aqueous solution, at room temperature, but decomposes in the synthetic reactant mixture at above 70 °C, suggesting that it is an unlikely intermediate in the formation of M41S structures.

Both the as-synthesized CTMA cubic octamer (Figure 13) and Q8M8 (Figure 13, insert) showed a distinct absorption band in the infrared near 580 cm^{-1}. This band is commonly found in zeolites which possess SBUs such as D4R.[40] This band has been recently assigned to an internal O−Si−O vibration using normal coordinate in the highly symmetric H form of the cubic octamer.[41,42] In addition to the Na and H forms of the

(28) Groenen, E. J. J.; Emeis, C. A.; van den Berg, J. P.; de Jong-Versloot, P. C. *Zeolites* **1987**, *7*, 474−77.
(29) Dutta, P. K.; Shieh, D. C. *J. Raman Spectrosc.* **1985**, *16*, 312.
(30) Smolen, Y. U. In *Soluble Silicates*; Falcone, Jr., J. S., Ed.; ACS Symposium Series 194, 1982, American Chemical Society: Washington, D. C.
(31) Harris, R. K.; Knight, C. T. G. *J. Mol. Struct.* **1982**, *78*, 273−78.
(32) Hasegawa, I.; Sakka, S. *Chem. Lett.* **1988**, 1319−22.
(33) Hoebbel, V. D.; Wieker, W. *Z. Anorg. Allg. Chem.* **1971**, *384*, 43−52.
(34) Engelhardt, G.; Hoebbel, D. *Z. Chem.* **1983**, *23*, 33.
(35) Ray, N. H.; Plaisted, R. J. *J. Chem. Soc., Dalton Trans.* **1983**, 475−81.
(36) Knight, C. T. G.; Kirpatrick, R. J.; Oldfield, E. *J. Chem. Soc., Chem. Commun.* **1986**, 66−67.
(37) Groenen, E. J. J.; Kortbeek, A. G. T. G.; Machay, M.; Sudmeijer, O. *Zeolites* **1986**, *6*, 403−11.
(38) Boxhoorn, G.; Sudmeijer, O.; van Kasteren, P. H. G. *J. Chem. Soc., Chem. Commun.* **1983**, 1416−1418.
(39) Knight, C. T. G. *Zeolites* **1990**, *10*, 140−144.
(40) Flanigen, E. M.; Khatami, H.; Syzanti, A. In *Adv. Chem. Series*; Gould, R. F., Ed.; American Chemical Society: Washington DC, 1971; p 210.
(41) Bornhauser, P.; Calzaferri, G. *Spectrochim. Acta* **1990**, *46A*, 1045.
(42) Bärtsch, M.; Bornhauser, P.; Bürgy, H.; Calzaferri, G. *Spectrochim. Acta* **1991**, *47A*, 1627−29.

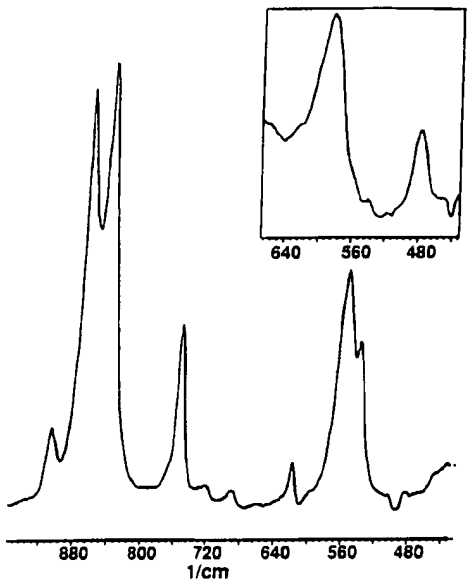

Figure 13. FTIR spectra of (A) as-synthesized CTMA cubic octamer and (B) (insert) recrystallized Q8M8 structure.

cubic octamer,[43] similar bands were reported in the tetramethylammonium silicates.[28,30-37]

CTMA silicate did lose the absorption band near 580 cm^{-1} when the FTIR sample was prepared as a pellet in a KBr matrix. A polyethylene matrix, however, gave satisfactory results. The trimethylsilylated derivative showed the band near 580 cm^{-1} even in the KBr matrix. These results seem to indicate that potassium ion exchange of the CTMA cation during mulling with solid KBr caused collapse of the D4R structure. This is consistent with the known sensitivity of the cubic octamer to the type and concentration of ammonium counterions.[44]

No absorption band in the "quartz gap" (500–650 cm^{-1}) was found for any of the M41S materials. This suggests that symmetric frameworks such as the D4R structure are not present in M41S materials and is consistent with the NMR data, which indicate that the octamer is unstable at typical M41S synthesis temperatures.

Mechanistic Considerations. The products formed in this simple synthesis system support the basic proposed liquid-crystal templating mechanism for the formation of M41S type materials. Three of the products, MCM-41 (hexagonal), MCM-48 (cubic), and the lamellar material mimic known liquid-crystal surfactant phases. The lack of stability of the cubic octamer at M41S synthesis temperatures make this compound an unlikely intermediate. The absence of any basic structural units in either NMR or FTIR analyses support this conclusion. However, the presence of this organosilicate and its stability, relative to other quaternary silicate structures, suggests that there exists a high affinity of the surfactant molecule for the silicate species. These data and the fact that MCM-41, MCM-48, and the lamellar phase can be formed in the same synthesis system by varying the silica concentration strongly support the proposed pathway B, in which the silicate anions (counterions) influence the formation of the various liquid-crystal templates.

Table 5. Effect of Various Anions on the Formation of Liquid-Crystal Phases for the Cetyltrimethylammonium System at 25 °C[a]

	wt % surfactant		
anion	hexagonal	cubic	lamellar
Cl^-	40–70	70–80	>80[a]
Br^-	20–65	>80[a]	>80[a]
SO_4^{2-}	50–65	40–45	

[a] T = >40 °C.

The ability of various counterions to influence the formation of liquid-crystal phases in surfactant systems is well documented in the literature. Variation in the counterion can influence whether a given liquid-crystal phase will form and at what surfactant concentration. The data presented in Table 5 illustrates the effect of different anions on the formation of liquid-crystal phases for the cetyltrimethylammonium system at 25 °C. For example, the hexagonal phase is favored over a wider and lower concentration range for the bromide containing system than for the chloride containing system.[16,46] The cubic phase forms in the sulfate-containing system at lower surfactant concentration than the hexagonal phase.[47] In a similar fashion, we believe that the silicate anions present in the M41S type preparations influence the formation of the various M41S phases that mimic known liquid-crystal phases. However, for the silicate system, these phase formations take place at relatively low surfactant concentration (~20–26 wt %). In the case of the silicate containing system, the anion (silicate) has the ability to form extended oligomers that result in the formation of stable inorganic structures MCM-41 (hexagonal), MCM-48 (cubic), and the lamellar phase.

The presence of alcohol is known to disrupt the formation of liquid-crystal phases in CTMA-containing solutions.[47] Ethanol can disrupt the hexagonal liquid-crystal phase at weight percentages of between 10 and 40% depending on the amount of surfactant in solution (~30–60%). However, in the M41S silicate/surfactant system, ethanol, generated in situ by the hydrolysis of TEOS, apparently does not have the same effect. For the MCM-41 preparation, the amount of ethanol generated could be as high as 50 wt % based on 4 mol of ethanol/mol of TEOS. In fact, all three liquid-crystal phases, hexagonal, cubic, and lamellar, were formed in the presence of potentially substantial amounts of ethanol. This may suggest that the silicate precursor responsible for the formation of the M41S structures is formed quite rapidly and is unresponsive to subsequent solution chemistry changes.

The sequence in which the phases are formed in this system is also consistent with a liquid-crystal templating mechanism. In surfactant chemistry, the hexagonal phase is typically the most stable and is formed with the least amount of perturbation of the system. Only

(43) Borbely, G.; Beyer, H. K.; Karge, H. G.; Schweiger, W.; Brandt, A.; Bergk, K.-H. *Clays Clay Miner.* **1991**, *39*, 490.
(44) Benn, R.; Grondey, H.; Brevard, C.; Pagelot, A. *J. Chem. Soc., Chem. Commun.* **1988**, 102–104.
(45) For a normal-coordinate analysis treatment of this region in zeolites see: van Santan, R. A.; Vogel, D. L. *Advances in Solid State Chemistry*; JAI Press: Greenwich, CT, 1989; p 151.
(46) Henriksson, U.; Blackmore, E. S.; Tiddy, G. J. T.; Soderman, O. *J. Phys. Chem.* **1992**, *96*, 3894–3902.
(47) Fontell, K.; Khan, B.; Lindstrom, K. B.; Maciejewska, D.; Puang-Ngern, S. *Colloid Polym. Sci.* **1991**, *269*, 727–42.

when the surfactant concentration, or other additives, are in greater concentration do the cubic and lamellar phases form.[15] In the M41S system, MCM-41 is formed with the highest concentration of silica, i.e., lowest Sur/Si ratio. The other two phases are formed at progressively higher Sur/Si ratios. Since the surfactant concentration for this system is below the concentration, where liquid-crystal structures typically appear,[4] pathway B seems a likely route for the formation of these new materials.

Recently, Monnier et al.[25] and Chen et al.[48] have explored the details of the liquid-crystal templating mechanism we first proposed.[1,3] These workers suggest that the precursor to the hexagonal member of the M41S family is either a lamellar phase[25] or a collection of individually silicated surfactant rods.[48] In both of these proposed mechanisms, the intermediates are silicate clad structures which are consistent with the proposed silicate initiated pathway. The transformation from a lamellar precursor to the hexagonal MCM-41 structure proposed by Monnier et al. appears plausible.[25] However, the transformation from this layered semicondensed silicate structure to a multidimensional structure for the cubic phase is more difficult to envision, unless this transformation from the lamellar phase to the hexagonal or cubic phase occurs quite rapidly and involves essentially bilayers of silicate/surfactant species. Both the cubic structure (i.e., bicontinuous) and a lamellar structure could be constructed from a bilayer precursor to represent the appropriate liquid-crystal phases and their M41S counterparts.

The formation of hexagonal, cubic, and lamellar structures using the proposed individual silicated surfactant rods also appears feasible.[48] As stated earlier, one of the proposed structures of the cubic liquid-crystal phase consists of intertwined surfactant rods.[20] A lamellar structure could also be constructed by stacking these same silicated rods directly on top of each other (a slight variation from the hexagonal packing needed for the MCM-41 formation). In either proposed intermediate, it is a silicated species that is responsible for the formation of the M41S structures, and there are subtle reaction variables responsible for the transformation between the three isolated phases (hexagonal, cubic, and lamellar). Our work suggests that this transformation is highly dependent on the surfactant to silica ratio, namely, at Sur/Si molar ratio <1 the hexagonal phase is made directly. At slightly higher values (Sur/Si 1−1.5), the cubic phase is obtained; at Sur/Si 1.2−2 the lamellar phase dominates.

(48) Chen, C. Y.; Burkett, S. L.; Li, H. X.; Davis, M. E. *Microporous Mater.* **1993**, *2*, 27−34.

Conclusions

The surfactant-to-silica molar ratio is a critical variable in the formation of liquid-crystal templated M41S materials. As this ratio was increased from 0.5 to 2.0, the siliceous products exhibited XRD patterns that are consistent with liquid-crystal phase transformations. These products exhibit hexagonal, cubic, and lamellar structures which mimic well-known liquid-crystal phases. The formation of these structures support the proposed mechanistic pathway in which M41S type materials form via a silicate anion induced liquid-crystal phase. Although the cubic octamer was also isolated in this same synthetic system, its lack of thermal stability at synthesis temperatures used for the formation of M41S materials suggest that this D4R structure is an unlikely intermediate or building unit of the silicate wall.

Acknowledgment. The authors are grateful to the staff at Mobil's Central and Paulsboro Research Laboratories for their invaluable discussion and effort. In particular, we acknowledge C. D. Chang, R. M. Dessau, and H. M. Princen for alerting us to references in the surfactant literature and helpful discussions on surfactant liquid crystal phases. We thank S. L. Laney, N. H. Goeke, H. W. Solberg, J. A. Pearson, and C. Martin for their expert technical assistance and J. B. Higgins for helpful technical discussions. We also thank Mobil Research and Development Corp. for its support.

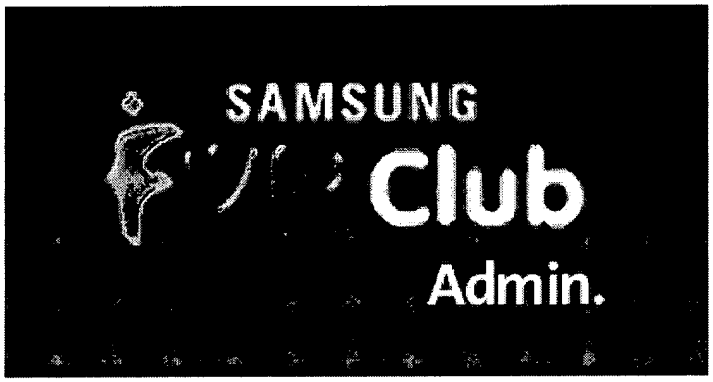

username

password

Login

Appendix II

Journal Home | ASAP Articles | Search Journals

journals & magazines
about the journal
ethical guidelines
sample issue
hot articles
special editorial
masthead
supporting info
author index
licensing info
how to subscribe
ACS Paragon System
info for authors
submit manuscript
info for reviewers
submit review
comments
info for reviewers
submit review
advertising info
copyright info
contacts/help
editorial office
customer service
technical support
e-mail webmaster
site map

ACS Pubs / ChemPort
CAS / chemistry.org

Table of Contents

Journal of The American Chemical Society

ASAP Articles
Issue: Previous / Next

Select Decade: 2000-Current | Select Volume: 2000/Vol 122 | Select Issue Number: Iss. 43/(10493-10742) | Go

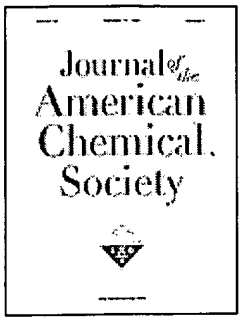

Journal of the American Chemical Society is the world's most respected chemical journal documenting advances in all areas of chemical research.

Display printer-friendly version

Journal of the American Chemical Society Table of Contents Vol. 122, No. 43: November 1, 2000

| Feedback | $ Purchase

New Insights into the Mechanism of CDP-D-Tyvelose 2-Epimerase: An Enzyme-Catalyzing Epimerization at an Unactivated Stereocenter
Tina M. Hallis, Zongbao Zhao, and Hung-wen Liu
pp 10493 - 10503; **(Article)** DOI: 10.1021/ja0022021

Abstract Full: HTML / PDF (159K)

| Feedback | $ Purchase

Crystal Structures of Substrate and Inhibitor Complexes with AmpC β-Lactamase: Possible Implications for Substrate-Assisted Catalysis
Alexandra Patera, Larry C. Blaszczak, and Brian K. Shoichet
pp 10504 - 10512; **(Article)** DOI: 10.1021/ja001676x

Abstract Full: HTML / PDF (777K)

| Feedback | $ Purchase

Flexible Structure of DNA: Ion Dependence of Minor-Groove Structure and Dynamics
Donald Hamelberg, Lori McFail-Isom, Loren Dean Williams, and W. David Wilson
pp 10513 - 10520; **(Article)** DOI: 10.1021/ja000707l

Abstract Full: HTML / PDF (229K) Supporting Info

| Feedback | $ Purchase

Enantioselective Total Synthesis of Epothilones A and B Using Multifunctional Asymmetric Catalysis
Daisuke Sawada, Motomu Kanai, and Masakatsu Shibasaki
pp 10521 - 10532; **(Article)** DOI: 10.1021/ja002024b

Abstract Full: HTML / PDF (197K) Supporting Info

| Feedback | $ Purchase

C_5Me_5/ER-Ligated Samarium(II) Complexes with the Neutral "C_5Me_5M" Ligand (ER = OAr, SAr, NRR', or PHAr; M = K or Na): A Unique Catalytic System for Polymerization and Block-Copolymerization of Styrene and Ethylene
Zhaomin Hou, Yugen Zhang, Hiroaki Tezuka, Peng Xie, Oliver Tardif, Take-aki Koizumi, Hiroshi Yamazaki, and Yasuo Wakatsuki
pp 10533 - 10543; **(Article)** DOI: 10.1021/ja002305j

Abstract Full: HTML / PDF (191K) Supporting Info

| Feedback | $ Purchase

Nickel L-Edge Soft X-ray Spectroscopy of Nickel-Iron Hydrogenases and Model Compounds-Evidence for High-Spin Nickel(II) in the Active Enzyme
Hongxin Wang, C. Y. Ralston, D. S. Patil, R. M. Jones, W. Gu, M. Verhagen, M. Adams, P. Ge, C. Riordan, C. A. Marganian, P. Mascharak, J. Kovacs, C. G. Miller, T. J. Collins, S. Brooker, P. D. Croucher, Kun Wang, E. I. Stiefel, and S. P. Cramer
pp 10544 - 10552; **(Article)** DOI: 10.1021/ja000945g

Abstract Full: HTML / PDF (114K)

| Feedback | $ Purchase

Characterization of Heterogeneous Nickel Sites in CO Dehydrogenases from *Clostridium thermoaceticum* and *Rhodospirillum rubrum* by Nickel L-Edge X-ray Spectroscopy
C. Y. Ralston, Hongxin Wang, S. W. Ragsdale, M. Kumar, N. J. Spangler, P. W. Ludden, W. Gu, R. M. Jones, D. S. Patil, and S. P. Cramer
pp 10553 - 10560; **(Article)** DOI: 10.1021/ja0009469

Abstract Full: HTML / PDF (130K) Supporting Info

| Feedback | $ Purchase

Synthesis and Characterization of Cross-Bridged Cyclams and Pendant-Armed Derivatives and Structural Studies of Their Copper(II) Complexes
Edward H. Wong, Gary R. Weisman, Daniel C. Hill, David P. Reed, Mark E. Rogers, Jeffrey S. Condon, Maureen A. Fagan, Joseph C. Calabrese, Kin-Chung Lam, Ilia A. Guzei, and Arnold L. Rheingold
pp 10561 - 10572; **(Article)** DOI: 10.1021/ja001295j

Abstract Full: HTML / PDF (172K) Supporting Info

| Feedback | $ Purchase

Titanium and Zirconium $Et_2C_2B_4H_4$-Metal-Phosphine Complexes: Synthesis, Characterization, and Ethylene Polymerization Activity
Tye Dodge, Michael A. Curtis, J. Monte Russell, Michal Sabat, M. G. Finn, and Russell N. Grimes
pp 10573 - 10580; **(Article)** DOI: 10.1021/ja001366e

Abstract Full: HTML / PDF (119K) Supporting Info

| Feedback | $ Purchase

Aqua, Alcohol, and Acetonitrile Adducts of Tris(perfluorophenyl)borane: Evaluation of Br Ø nsted Acidity and Ligand Lability with Experimental and Computational Methods
Catherine Bergquist, Brian M. Bridgewater, C. Jeff Harlan, Jack R. Norton, Richard A. Friesner, and Gerard Parkin
pp 10581 - 10590; **(Article)** DOI: 10.1021/ja001915g

Abstract Full: HTML / PDF (159K) Supporting Info

| Feedback | $ Purchase

TEM and Laser-Polarized ^{129}Xe NMR Characterization of Oxidatively Purified Carbon Nanotubes
J. M. Kneller, R. J. Soto, S. E. Surber, J.-F. Colomer, A. Fonseca, J. B. Nagy, G. Van Tendeloo, and T. Pietra
pp 10591 - 10597; **(Article)** DOI: 10.1021/ja994441y

Abstract Full: HTML / PDF (350K)

| Feedback | $ Purchase

Copper(II)-Assisted Enantiomeric Analysis of D,L-Amino Acids Using the Kinetic Method: Chiral Recognition and Quantification in the Gas Phase
W. A. Tao, Duxi Zhang, Eugene N. Nikolaev, and R. Graham Cooks
pp 10598 - 10609; **(Article)** DOI: 10.1021/ja000127o

Abstract Full: HTML / PDF (138K) Supporting Info

| Feedback | $ Purchase

A Role for Induced Molecular Polarization in Catalytic Promotion: CO Coadsorbed with K on Co {10$\bar{1}$0}
Stephen J. Jenkins and David A. King
pp 10610 - 10614; **(Article)** DOI: 10.1021/ja0004985

Abstract Full: HTML / PDF (200K)

| Feedback | $ Purchase

Detection of Hydrophobic End Groups on Polymer Surfaces by Sum-Frequency Generation Vibrational Spectroscopy
Zhan Chen, Robert Ward, Yuan Tian, Steve Baldelli, Aric Opdahl, Yuen-Ron Shen, and Gabor A. Somorjai
pp 10615 - 10620; **(Article)** DOI: 10.1021/ja000808j

Abstract Full: HTML / PDF (124K)

| Feedback | $ Purchase

Ab Initio Study of the Electronic Excited States in 4-(*N,N*-Dimethylamino)benzonitrile with Inclusion of Solvent Effects: The Internal Charge Transfer Process
Benedetta Mennucci, Alessandro Toniolo, and Jacopo Tomasi
pp 10621 - 10630; **(Article)** DOI: 10.1021/ja000814f

Abstract Full: HTML / PDF (425K)

| Feedback | $ Purchase

Vibronic Structure and Coupling in the Electronic Spectra of the Hexacarbonyl Tantalate(I-) Ion
Theodore W. Bitner and Jeffrey I. Zink
pp 10631 - 10639; **(Article)** DOI: 10.1021/ja0010305

Abstract Full: HTML / PDF (127K)

| Feedback | $ Purchase

The Effect of Finite Sampling on the Determination of Orientational Properties: A Theoretical Treatment with Application to Interatomic Vectors in Proteins
David Fushman, Ranajeet Ghose, and David Cowburn
pp 10640 - 10649; **(Article)** DOI: 10.1021/ja001128j

Abstract Full: HTML / PDF (135K) Supporting Info

| Feedback | $ Purchase

Cyclic In-Plane Electron Delocalization (σ-Bishomoaromaticity) in 4N/5e Radical Anions and 4N/6e Dianions-Generation, Structures, Properties, Ion-Pairing, and Calculations
Kai Exner, Oliver Cullmann, Markus Vögtle, Horst Prinzbach, Birgit Grossmann, Jürgen Heinze, Lorenz Liesum, Rainer Bachmann, Arthur Schweiger, and Georg Gescheidt
pp 10650 - 10660; **(Article)** DOI: 10.1021/ja0014943

Abstract Full: HTML / PDF (253K) Supporting Info

Remarkable Conformational Control of Photoinduced Charge Separation and Recombination in a Giant U-Shaped Tetrad
Toby D. M. Bell, Katrina A. Jolliffe, Kenneth P. Ghiggino, Anna M. Oliver, Michael J. Shephard, Steven J. Langford, and Michael N. Paddon-Row
pp 10661 - 10666; **(Article)** DOI: 10.1021/ja001492i

Abstract Full: HTML / PDF (87K)

Bond Dissociation Energy in Trifluoride Ion
Alexander Artau, Katrina Emilia Nizzi, Brian T. Hill, Lee S. Sunderlin, and Paul G. Wenthold
pp 10667 - 10670; **(Article)** DOI: 10.1021/ja001613e

Abstract Full: HTML / PDF (56K)

Simple Model for Nonassociative Organic Liquids and Water
Peter Buchwald and Nicholas Bodor
pp 10671 - 10679; **(Article)** DOI: 10.1021/ja001788o

Abstract Full: HTML / PDF (112K) Supporting Info

Reactions of Group IV Metal Atoms with Water Molecules. Matrix Isolation FTIR and Theoretical Studies
Mingfei Zhou, Luning Zhang, Jian Dong, and Qizong Qin
pp 10680 - 10688; **(Article)** DOI: 10.1021/ja0020658

Abstract Full: HTML / PDF (156K)

Formation of Gas-Phase Dianions and Distonic Ions as a General Method for the Synthesis of Protected Reactive Intermediates. Energetics of 2,3- and 2,6-Dehydronaphthalene
Dana R. Reed, Michael Hare, and Steven R. Kass
pp 10689 - 10696; **(Article)** DOI: 10.1021/ja002351j

Abstract Full: HTML / PDF (108K)

The Electron as a Protecting Group. 2. Generation of Benzocyclobutadiene Radical Anion in the Gas Phase and an Experimental Determination of the Heat of Formation of Benzocyclobutadiene
Katherine M. Broadus and Steven R. Kass
pp 10697 - 10703; **(Article)** DOI: 10.1021/ja002352b

Abstract Full: HTML / PDF (99K)

Porphyrin-Fullerene Host-Guest Chemistry
Dayong Sun, Fook S. Tham, Christopher A. Reed, Leila Chaker, Michael Burgess, and Peter D. W. Boyd
pp 10704 - 10705; **(Communication)** DOI: 10.1021/ja002214m

Full: HTML / PDF (53K) Supporting Info

Isospecific Living Polymerization of 1-Hexene by a Readily Available Nonmetallocene C_2-

Symmetrical Zirconium Catalyst
Edit Y. Tshuva, Israel Goldberg, and Moshe Kol
pp 10706 - 10707; **(Communication)** DOI: 10.1021/ja001219g

Full: HTML / PDF (38K) Supporting Info

| Feedback | $ Purchase

Total Synthesis and Absolute Structure of Manzacidin A and C
Kosuke Namba, Tetsuro Shinada, Toshiyuki Teramoto, and Yasufumi Ohfune
pp 10708 - 10709; **(Communication)** DOI: 10.1021/ja002556s

Full: HTML / PDF (47K) Supporting Info

| Feedback | $ Purchase

Lewis Acid-Catalyzed Enantioselective 1,3-Dipolar Cycloadditions of Diazoalkane: Chiral Ligand/Achiral Auxiliary Cooperative Chirality Control
Shuji Kanemasa and Toshio Kanai
pp 10710 - 10711; **(Communication)** DOI: 10.1021/ja002670a

Full: HTML / PDF (37K) Supporting Info

| Feedback | $ Purchase

Synthesis of New, Nanoporous Carbon with Hexagonally Ordered Mesostructure
Shinae Jun, Sang Hoon Joo, Ryong Ryoo, Michal Kruk, Mietek Jaroniec, Zheng Liu, Tetsu Ohsuna, and Osamu Terasaki
pp 10712 - 10713; **(Communication)** DOI: 10.1021/ja002261e

Full: HTML / PDF (69K)

| Feedback | $ Purchase

A Novel Copper-Mediated DNA Base Pair
Eric Meggers, Patrick L. Holland, William B. Tolman, Floyd E. Romesberg, and Peter G. Schultz
pp 10714 - 10715; **(Communication)** DOI: 10.1021/ja0025806

Full: HTML / PDF (34K) Supporting Info

| Feedback | $ Purchase

Rhodium-Catalyzed Asymmetric Conjugate Addition of Organoboronic Acids to Nitroalkenes
Tamio Hayashi, Taichi Senda, and Masamichi Ogasawara
pp 10716 - 10717; **(Communication)** DOI: 10.1021/ja002805c

Full: HTML / PDF (37K) Supporting Info

| Feedback | $ Purchase

Unusual in Situ Ligand Modification to Generate a Catalyst for Room Temperature Aromatic C-O Bond Formation
Quinetta Shelby, Noriyasu Kataoka, Grace Mann, and John Hartwig
pp 10718 - 10719; **(Communication)** DOI: 10.1021/ja002543e

Full: HTML / PDF (44K) Supporting Info

| Feedback | $ Purchase

Synthesis, Structure, and Magnetic Properties of a New Ternary Zintl Phase: $Sr_{21}Mn_4Sb_{18}$
Hyungrak Kim, Cathie L. Condron, Aaron P. Holm, and Susan M. Kauzlarich
pp 10720 - 10721; **(Communication)** DOI: 10.1021/ja002709b

Full: HTML / PDF (60K) Supporting Info

| Feedback | $ Purchase

Incorporation of N_2 and CO into Organic Molecules: Amide Formation by Palladium-Catalyzed Carbonylation and Nitrogenation
Kazutaka Ueda, Yoshihiro Sato, and Miwako Mori
pp 10722 - 10723; **(Communication)** DOI: 10.1021/ja002707r

Full: HTML / PDF (34K) Supporting Info

| Feedback | $ Purchase

A Molecular Dynamics Test of the Different Stability of Crystal Polymorphs under Thermal Strain
A. Gavezzotti
pp 10724 - 10725; **(Communication)** DOI: 10.1021/ja000588+

Full: HTML / PDF (29K)

| Feedback | $ Purchase

Methylbenzenes Are the Organic Reaction Centers for Methanol-to-Olefin Catalysis on HSAPO-34
Weiguo Song, James F. Haw, John B. Nicholas, and Catherine S. Heneghan
pp 10726 - 10727; **(Communication)** DOI: 10.1021/ja002195g

Full: HTML / PDF (27K)

| Feedback | $ Purchase

A Fundamentally New Approach to Enantioselective Fluorination Based on Cinchona Alkaloid Derivatives/Selectfluor Combination
Norio Shibata, Emiko Suzuki, and Yoshio Takeuchi
pp 10728 - 10729; **(Communication)** DOI: 10.1021/ja002732x

Full: HTML / PDF (33K) Supporting Info

| Feedback | $ Purchase

Control of Photonic Band Structure by Molecular Aggregates
Zhong-Ze Gu, Sinya Hayami, Qing-Bo Meng, Tomokazu Iyoda, Akira Fujishima, and Osamu Sato
pp 10730 - 10731; **(Communication)** DOI: 10.1021/ja001868s

Full: HTML / PDF (43K)

| Feedback | $ Purchase

Mechanism of Glutamate Mutase: Identification and Kinetic Competence of Acrylate and Glycyl Radical as Intermediates in the Rearrangement of Glutamate to Methylaspartate
Hung-Wei Chih and E. Neil G. Marsh
pp 10732 - 10733; **(Communication)** DOI: 10.1021/ja002488+

Full: HTML / PDF (29K)

| Feedback | $ Purchase

S-Nitrosylation of Cross-Linked Hemoglobins at β-Cysteine-93: Stabilized Hemoglobins as Nitric Oxide Sources
John Paul Pezacki, Andrew Pelling, and Ronald Kluger
pp 10734 - 10735; **(Communication)** DOI: 10.1021/ja005516x

Full: HTML / PDF (56K)

| Feedback | $ Purchase

Migrating Alkynes in Vinylidene Carbenoids: An Unprecedented Route to Polyynes
Sara Eisler and Rik R. Tykwinski
pp 10736 - 10737; **(Communication)** DOI: 10.1021/ja005557t

Full: HTML / PDF (31K) Supporting Info

Feedback | $ Purchase

Protein Flexibility Correlates with Degree of Hydrogen Tunneling in Thermophilic and Mesophilic Alcohol Dehydrogenases
Amnon Kohen and Judith P. Klinman
pp 10738 - 10739; **(Communication)** DOI: 10.1021/ja002229k

Full: HTML / PDF (87K)

Feedback | $ Purchase

Insights into Metal Framework Constructions from the Syntheses of New Scandium- and Yttrium-Rich Telluride Compounds: $Y_5Ni_2Te_2$ and Sc_6PdTe_2
Paul A. Maggard and John D. Corbett
pp 10740 - 10741; **(Communication)** DOI: 10.1021/ja002875j

Full: HTML / PDF (188K) Supporting Info

BOOK REVIEWS

Feedback | $ Purchase

Metal-Organic and Organic Molecular Magnets Edited by P. Day (The Royal Institution of Great Britain) and A. E. Underhill (University College of North Wales). Royal Society of Chemistry: Cambridge. 1999. viii + 324 pp. £69.50. ISBN 0-85404-764-6

pp 10742 - 10742; **(Book Review)** DOI: 10.1021/ja004773z

Full: HTML / PDF (10K)

Feedback | $ Purchase

Indirect Food Additives and Polymers: Migration and Toxicology By Victor O. Sheftel (Ministry of Health, State of Israel, Jerusalem). Lewis Publishers: Boca Raton, FL. 2000. xvi + 1304 pp. $129.95. ISBN 1-56670-499-5.

pp 10742 - 10742; **(Book Review)** DOI: 10.1021/ja004778w

Full: HTML / PDF (10K)

Feedback | $ Purchase

Methods in Molecular Biology. Volume 146. Mass Spectrometry of Proteins and Peptides Edited by John R. Chapman (Sale, Manchester, UK). Humana Press: Totowa, NJ. 2000. xiv + 538 pp. $125.00. ISBN 0-896-03609-X

pp 10742 - 10742; **(Book Review)** DOI: 10.1021/ja004779o

Full: HTML / PDF (10K)

Feedback | $ Purchase

Chemistry of Atmospheres. An Introduction to the Chemistry of the Atmospheres of Earth, the Planets, and Their Satellites. Third Edition By Richard P. Wayne (University of Oxford). Oxford University Press: Oxford. 2000. xxx + 776 pp. $57.95. ISBN 0-19-850375-X

pp 10742 - 10742; **(Book Review)** DOI: 10.1021/ja004780n

Full: HTML / PDF (10K)

| Feedback | $ Purchase

Quantum Chemistry. Classic Scientific Papers. World Scientific Series in 20th Century Chemistry. Volume 8 Translated and edited by Hinne Hettema (University of Auckland). World Scientific: Singapore; River Edge, NJ; London; Hong Kong. 2000. xxxx + 478 pp. $90.00. ISBN 981-02-2771-X

pp 10742 - 10742; **(Book Review)** DOI: 10.1021/ja004781f

Full: HTML / PDF (10K)

| Feedback | $ Purchase

Contemporary Boron Chemistry Edited by M. G. Davidson (University of Bath), Andrew K. Hughes, Todd B. Marder, and Ken Wade (University of Durham). Royal Society of Chemistry: Cambridge. 2000. xvi + 538 pp. $199.00. ISBN 0-85404-835-9.

pp 10742 - 10742; **(Book Review)** DOI: 10.1021/ja0047875

Full: HTML / PDF (10K)

| Feedback | $ Purchase

Phosphorus 2000. Chemistry, Biochemistry and Technology By D. E. C. Corbridge (Harrogate, UK). Elsevier: Amsterdam. 2000. x + 1258 pp. $573.50. ISBN 0-444-82550-9.

pp 10742 - 10742; **(Book Review)** DOI: 10.1021/ja004788x

Full: HTML / PDF (10K)

▲ Page Top

▶ Please Note: Acrobat Reader 4.0 or higher is recommended for viewing PDF files.